Korean J. Chem. Eng., **29**(6), 737-742 (2012)
DOI: 10.1007/s11814-011-0238-7

A model on chemical looping combustion of methane in a bubbling fluidized-bed process

Jeong-Hoo Choi*,†, Pil Sang Youn*, Djamila Brahimi*, Young-Wook Jeon, Sang Done Kim***, and Ho-Jung Ryu******

*Department of Chemical Engineering, Konkuk University, Seoul 143-701, Korea
**SK Innovation, Daejeon 305-712, Korea
***Department of Chemical & Biomolecular Engineering and Energy & Environment Research Center, KAIST, Daejeon 305-701, Korea
****Korea Institute of Energy Research, Daejeon 305-343, Korea
(*Received 1 June 2011 • accepted 9 September 2011*)

Abstract–We developed a mathematical model to discuss the performance of chemical looping combustion (CLC) of methane in continuous bubbling fluidized-beds. The model considers the particle population balance, oxidation and reduction rate of particles in fluidized beds. It also considers utilization efficiency of oxygen carrier (OC) particles, residence time of particles in each reactor, and particle size in reaction rate. The model was applied for a bubbling core-annulus fluidized-bed process. The core bed was the fuel reactor (0.08 m-i.d., 2.1 m-height) and the annulus bed was the air reactor (0.089 m-i.d., 0.15 m-o.d., 1.6 m-height). The process employed a type of Ni-based OC particles. The present model agrees reasonably well with the combustion efficiency measured in the process. Simulation was performed to investigate the effects of some variables for the process. The present model revealed that the range of circulation rate of OC particles for achieving complete combustion determined the operating range of the CLC system. The minimum circulation rate of OC particles for complete combustion decreased in the considered operating range as temperature or bed mass increased in the fuel reactor. A large mass of the fuel bed was necessary to obtain complete combustion at low fuel reactor temperature. The fresh feed rate of OC particles for steady state operation increased in complete combustion condition as temperature or static bed height or gas velocity increased.

Key words: Model, Chemical Looping Combustion, CLC, Fluidized Bed, Methane

INTRODUCTION

CO_2 capture from flue gas has become one of the important issues to prevent global warming. The chemical looping combustion (CLC) method draws much attention because it can separate CO_2 produced in the combustion system. The chemical looping combustion system consists of a fuel reactor and an air reactor. In the fuel reactor, the fuel is oxidized by metal oxide particles producing almost pure CO_2 and H_2O, leading to easy and inexpensive carbon sequestration [1]. The reduced oxide particles are then transported to the air reactor, where air is used to oxidize the solid particles. The fuel has little contact with air directly in the CLC system and thereby formation of harmful NO_x gases can be almost prevented. The sum of the heat generated or consumed in the reduction stage and the heat generated in the oxidation stage is equal to the heat generated by direct oxidation of the fuel gas.

The CLC system is well acknowledged to be a very complicated system because the oxygen is supplied by oxygen carrier (OC) particles circulating between fuel and air reactors that interact with each other. Development of a mathematical model on the system provides a convenient tool for investigating the effects of various operating parameters on the reactor performance in advance. It is also good to save money and effort in systematic understanding of the experimental result, design and operation. Some models on analysis of the process have been reported [1-10]. Balaji et al. [1] developed a model based on system invariants under thermodynamic equilibrium to propose a control-oriented model for transient and steady-state conditions. They assumed that the particle size would unchange and the reactive core size would shrink by the shrinking-core mechanism. They considered CH_4 as fuel and Fe_2O_3 as oxygen carrier. Deng et al. [2,7] developed a computational fluid dynamic (CFD) model on the fuel reactor using single size $CaSO_4$ particles as oxygen carrier for H_2. The effect of particle diameter was obvious on CLC performance. They did not include the cyclone in the system. Jung and Gamwo [3] developed a CFD model on the fuel reactor with single-size NiO particles as oxygen carrier and CH_4 as fuel. They did not consider the cyclone in the system. Abad et al. [4,5] developed a model to simulate the performance of the steady-state fuel reactor in CLC system that considered CH_4 for fuel and single-size $CuO-Al_2O_3$ particles as oxygen carrier. Their model focused on the fuel reactor with solid conversion of the air reactor given as a parameter. CH_4 conversion was highly dependent on the solid conversion of the air reactor. Bolhàr-Nordenkampf et al. [6] developed a thermodynamic equilibrium model on the CLC system, based on conservation of mass and energy. The model considered few fluidizing behaviors of particles in both reactors. Iliuta et al. [9] developed a transient model to investigate kinetic behaviors of the fuel reactor. They considered CH_4 as fuel and NiO as oxygen carrier. Kolbitsch et al. [8] developed a model for a dual circulating-fluidized-bed CLC system. They used a simple parameter named the fraction of solids exposed to gas passing in plug flow to characterize the gas-solid contact. They considered single size NiO particles as oxygen carrier and natural gas as fuel. Kruggel-Emden et al. [10]

†To whom correspondence should be addressed.
E-mail: choijhoo@konkuk.ac.kr

developed a transient CFD model to simulate the start-up period of the CLC system for 60 s. They considered no cyclones in the system, CH_4 as fuel and single-size Mn_3O_4 particles as oxygen carrier. However, few of the past models considered particle-side factors in fuel and air reactors together in steady-state condition such as wide-size distribution, attrition, formation of fine particles by attrition, resultant loss of fine particles by elutriation, and makeup of fresh particles.

The purpose of this study is to build a practical model to discuss performance of CLC of methane in a bubbling fluidized bed at steady state. Ni-based particles were employed as oxygen carrier. The model considered the particle population balance, oxidation, and reduction rate of particles in fuel and air reactors. It also considered utilization efficiency of oxygen carrier particles, residence time of particles in each reactor, and particle size in reaction rate. The model was applied for a bubbling core-annulus fluidized-bed CLC process to discuss the operating condition.

MODEL

Fig. 1 shows the schematic diagram of the process considered in this study, which uses bubbling-bed fuel and air reactors. The process can be described as follows: CH_4 gas is introduced to the fuel reactor and fluidizes the bed of oxygen carrier (OC) particles; methane burns according to the following reaction: $CH_4(g)+4NiO(s) \rightarrow CO_2(g)+2H_2O(g)+4Ni(s)$; The product gas, including elutriated particles, is sent to the cyclone separator; a certain fraction of particles collected in the cyclone are returned to the fuel reactor; reacted particles are withdrawn from the bottom of the fuel reactor and fed to the air reactor; oxidant gas containing O_2 is introduced to the air reactor and fluidizes the bed of OC particles; Ni in particles is oxidized according to the following reaction: $Ni(s)+1/2\ O_2(g) \rightarrow NiO(s)$; oxidized carrier particles are withdrawn from the bottom of the air reactor and fed to the fuel reactor; and fresh OC particles are fed to the fuel reactor to make up for any loss of particles from the process.

In Fig. 1, F_j is the solid flow rate of stream j, x the spherical particle diameter, $p_j(x)$ probability density function of particles in stream j, $p_{bi}(x)$ probability density function of particles in bed i, W_i weight of bed i, $R_i(x)$ particle attrition rate in bed i, R_{ai} overall formation rate of fine particles by attrition in bed i, $K_i^*(x)$ particle elutriation rate from bed i, and $\psi_i(x)$ fractional particle collection efficiency of cyclone i. The fractional collection efficiency of the cyclone was assumed as that of Lapple [11]. We assumed a well-mixed state of bed particles in both reactors ($p_1(x)=p_{b1}(x)$, $p_{10}(x)=p_{b2}(x)$) and a constant apparent particle density.

The particle population balance in the fuel (i=1) and air (i=2) reactor at the steady state, considering the elutriation rate and attrition rate, is expressed as follows [12].

$$\frac{dp_{bi}(x)}{dx} + \alpha_{ik}(x)p_{bk}(x) - \alpha_{i3}(x) = 0 \quad (i=1,2;\ k=1,2) \tag{1}$$

$$\alpha_{i1}(x) = \delta_{1i}\left[\frac{F_1 + K_1^*(x)(1-\psi_1(x)R_{f12})}{W_1R_1(x)} + \frac{1}{R_1(x)}\frac{dR_1(x)}{dx} - \frac{3}{x}\right] - \delta_{2i}\frac{F_1}{W_2R_2(x)} \tag{2a}$$

$$\alpha_{i2}(x) = -\delta_{1i}\frac{F_{10}}{W_1R_1(x)} + \delta_{2i}\left[\frac{F_{10} + K_2^*(x)(1-R_{f2}\psi_2(x))}{W_2R_2(x)} + \frac{1}{R_2(x)}\frac{dR_2(x)}{dx} - \frac{3}{x}\right] \tag{2b}$$

$$\alpha_{i3}(x) = -\frac{\delta_{1i}F_0p_0(x) + R_{ai}p_{ai}(x)}{W_iR_i(x)} \tag{2c}$$

B. C.: $p_{bi}(x)=0$ for $x=x_{max}$, constraint: $\int_0^{x_{max}} p_{bi}(x)\,dx = 1$ (2d, e)

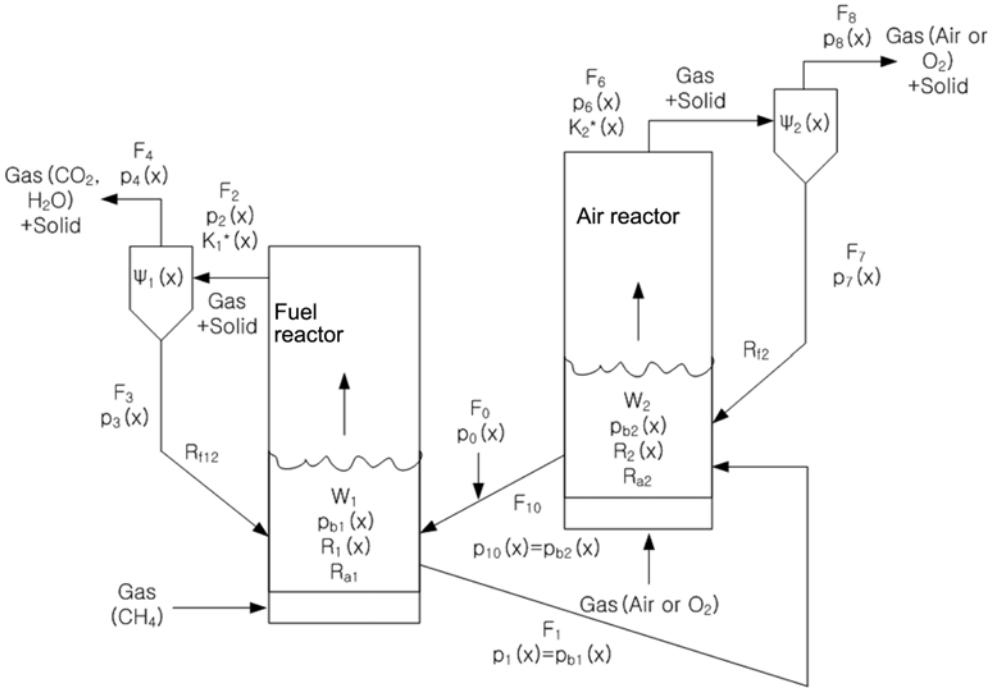

Fig. 1. Schematic diagram of a bubbling fluidized-bed CLC system.

x_{max} is the maximum particle diameter.

The fresh feed rate of OC particles F_0 and the circulation rate of OC particles F_{10} are controlled to maintain fixed values of F_1, W_1 and W_2 for the given fluidizing condition. Therefore, F_0 and F_{10} are determined to satisfy constraint (Eq. (2e)) in solving the particle population balances.

We used the correlations of Choi et al. [13] to calculate the particle elutriation rate, correlations which have been confirmed as providing reasonable accuracy in expressing the effects of temperature and pressure. We used the simple model of Merrick and Highley [14] to express the total formation rate of fine particles and size reduction rate of single particle by attrition in the fluidized bed as

$$R_{ai}=K_a(u_i-u_{mfi})W_i,\ R_i(x)=dx/dt=-K_a(u_i-u_{mfi})x/3 \quad (3a, b)$$

K_a is the particle attrition rate constant. We assumed that fine particles formed by abrasion were below 5 μm in diameter [15] and had a uniform size distribution. In addition, because the rate of size reduction as well as the retention time in the reactor is relatively very small, we assumed that there would be negligible particle attrition for particles below 5 μm in diameter. Minimum fluidizing velocity (u_{mfi}) was calculated from the correlation of Wen and Yu [16], based on the bed particle size distribution.

Based on experimental results from a thermo-gravimetric analyzer (TGA) [17] and a set of data from a steady state CLC system [18], kinetic equations of reduction reaction (i=1) and oxidation reaction (i=2) in reactors could be expressed in a form which incorporates Arrhenius' law as follows:

$$\frac{dX_i}{dt}=\frac{6\eta_i b_i k_{oi} e^{-E_i/RT_i}(C_i')^{n_i}}{\gamma_i x}(1-X_i)^{2/3} \quad (4)$$

The γ_i is mole of solid reactant per volume of particles in reactor i, b_1 is 4, b_2 is 2, k_{o1} is 8.224×10^{-3} $(kg\ mol)^{0.333}m^{0.001}/s$, k_{o2} is 2.625×10^{-2} $(kg\ mol)^{0.232}m^{0.304}/s$ E_1 is 1.859×10^4 J/g mol, E_2 is 2.312×10^4 J/g mol, n_1 is 0.667, n_2 is 0.768 [17]. The η_1 is 3.866×10^{-4} and η_2 is 2.586×10^{-3}. The η_1 and η_2 were factors compensating difference in reaction environment between the TGA [17] and the CLC system [18]. They were determined by fitting the present model to one of actual process data (F_{10}=10.01 g/s) shown in Fig. 2. The fraction of active Ni for oxygen carrier particles is influenced by CH_4 concentration and temperature in the fuel reactor [9]. The fraction of active Ni was defined as the fractional conversion of NiO to Ni when carbon deposition started during fuel combustion. It is represented by the following correlation [17].

$$\phi=0.02629e^{0.002463T_1}(C_1')^{-0.08465} \quad (5)$$

The particle reaction time in each reactor was assumed to be the mean particle residence time written as [12]

$$\tau_i(x)=W_i\omega_{bi}(x)/\sum_{outflow(j)}S_{ij}\omega_{ij}(x) \quad (6)$$

The average concentration of the gas reactant in each reactor was simply considered as an arithmetic mean value between inlet and outlet concentration.

$$C_i'=\frac{C_{i0}'+C_{if}'}{2} \quad (7)$$

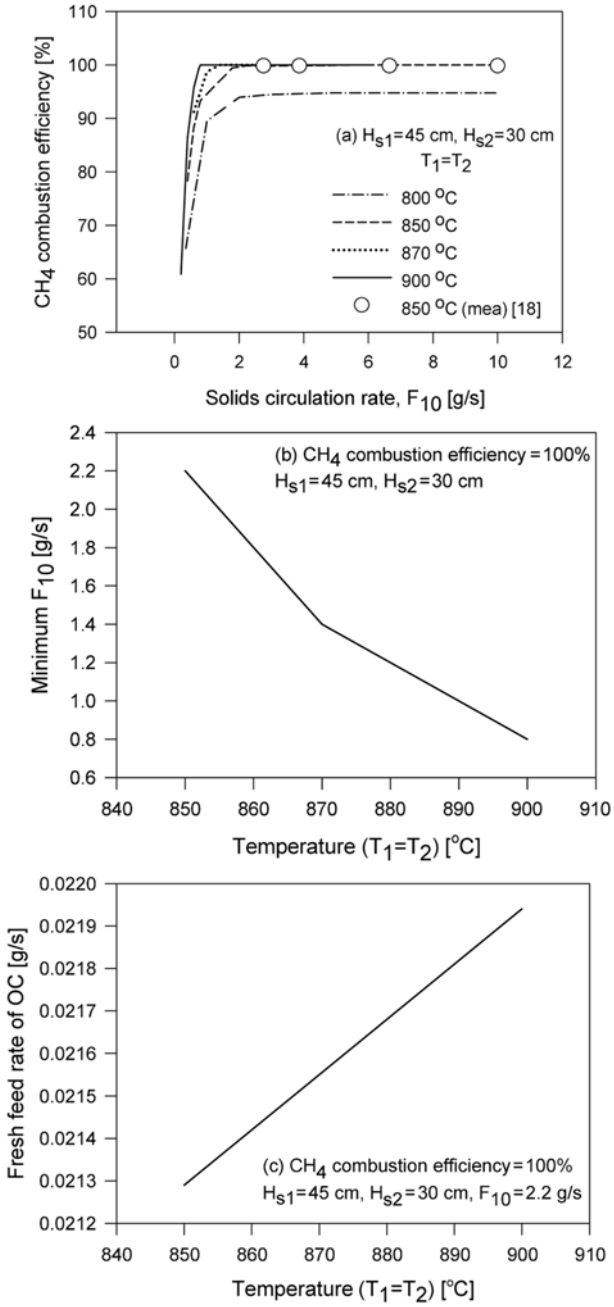

Fig. 2. Effect of temperature on performance of CLC (symbol: measured [18], lines: calculated by the present model).

The bed flow pattern seemed to change a little with variation of operating conditions in the same bubbling fluidization. Therefore, we think that present reaction rates (Eq. (4)) can be utilized reasonably for systems of different dimensions and/or some different operating conditions in the same bubbling regime. However, correction in reaction rates (Eq. (4)) should be considered in a different fluidization regime.

CALCULATION PROCEDURE

Mass flow rates and size distributions of all particle streams can be determined from combining population balances (Eqs. (1) and

(2)) by numerical method, whereby an initial educated guess for outlet concentration of CH_4 in the fuel reactor and O_2 in the air reactor is used to determine the consumption rate of each gas (Δm_{CH_4}, Δm_{O_2}) and the average concentration term of each gas as $(C_i')^n$ in the reactor, in turn. The NiO concentration of particles in each reactor is calculated as follows: 1) Make a best guess for NiO concentration of particles withdrawn from the air reactor. The particles are fed to the fuel reactor. 2) Evaluate NiO concentration of the particles when it is withdrawn from the fuel reactor after reaction time of mean residence time. The particles are returned to the air reactor. 3) Evaluate NiO concentration of the particles withdrawn from the air reactor after reaction time of mean residence time. 4) See if the difference between the calculated NiO concentration of the particle from the air reactor and the one initially guessed in step 1 is within tolerance. If not, go back to step 1 and make another educated guess from the results. Use the same calculation for all particle size. From this, we can obtain the total mole flow rate of oxygen (O_2) removed by CH_4 from the solid phase in the fuel reactor ($\Delta m_{NiO,1}$) and the total mole flow rate of oxygen (O_2) adsorbed from the gas phase to particles in the air reactor ($\Delta m_{NiO,2}$). The following relations between consumed moles of gaseous reactants (CH_4, O_2) and reacted moles of NiO (formed and then disappeared) must be satisfied in each reactor:

$$\Delta m_{NiO,1}=4\Delta m_{CH_4},\quad \Delta m_{NiO,2}=2\Delta m_{O_2} \tag{8a, b}$$

Continue with best guesses for outlet concentration of CH_4 in the fuel reactor and O_2 in the air reactor to narrow the differences until relations (8a, b) are satisfied within tolerance. The fluidizing gas velocity is considered as an arithmetic mean value between bottom and top of bed in iteration.

SIMULATION CONDITIONS

The present model was applied for a CLC process using bubbling core-annulus fluidized beds (fuel reactor, core bed: 0.08 m i.d., 2.1 m height; air reactor, annulus bed: 0.089 m-i.d., 0.15 m-o.d., 1.6 m-height) in the Korea Advanced Institute of Science and Technology (KAIST) [18]. To give safe residence time to particles in the bed, the inlet and the outlet of particles were placed in opposite sides of each reactor without any trouble in particle flow. The process used oxygen carrier particles Ni-based with 70 wt% NiO. Size distribution of fresh oxygen carrier particles was as follows in wt% for a size range: 7.49 wt% for 0-75 μm, 32.55 wt% for 75-105 μm, 32.91 wt% for 105-125 μm, 21.30 wt% for 125-150 μm, 5.75 wt% for 150-180 μm. Fuel gas fed to the fuel reactor was a mixture of 33.3% CH_4 and 66.7% N_2. Dry air was used as oxidant gas for the air reactor. Both reactors equipped with electric heaters were set same temperature. The apparent particle density was 2,788 kg/m^3. The simulation conditions were determined to discuss the possible operating conditions and effects of some principal variables for this process. We considered solid circulation rate, temperature and bed mass as model parameters. The following settings were held constant as experimental conditions of the KAIST process: reactor pressure, 101.3 kPa; cyclone cut diameter, 0.03 mm; K_a, 4.5×10^{-6} 1/m; feed gas velocity, 0.0372 m/s for the fuel reactor, 0.0817 m/s for the air reactor; excess oxygen, 57.7%; particles collected by cyclones were not recycled, $R_{f12}=R_{f2}=0$.

RESULTS AND DISCUSSION

Simulation was performed to discuss the operating condition and investigate effects of some variables for the process. Fig. 2(a) shows the methane combustion efficiency with respect to the solids circulation rate at various bed temperatures. The fuel and air reactor temperatures were considered the same. The excess O_2 was set 57.7%, based on the feed methane to the fuel reactor and oxygen supply to the air reactor. Static bed heights of fuel and air reactors were set 0.45 m and 0.3 m, respectively, as the experimental condition of the KAIST process. Lines represent values predicted by the present model, the symbol represents measured values in the KAIST process [18]. The combustion efficiency is predicted to increase as temperature or solids circulation rate increases. This result is attributed to the increase of reaction rate and fraction of active Ni in fuel reactor particles (Eqs. (4), (5)). The present result agrees with the results of Deng et al. [2,7] on the temperature effect and Abad et al. [4,5] and Kolbitsch et al. [8] on effects of temperature and solids circulation rate. However, the combustion efficiency did not appear to achieve 100% at temperature <850 °C with any solids circulation rate because the reaction rate and fraction of active Ni in fuel reactor particles decreased. The present model agrees reasonably well with measured values at 850 °C. The minimum solids circulation rate required for complete combustion in Fig. 2(b) decreased as temperature increased >850 °C [4,5]. The fresh feed rate of OC particles in Fig. 2(c) was predicted to increase a little in complete combustion condition as temperature increased, because the elutriation rate increases with an increase of temperature [13] in this range.

Fig. 3(a) shows the effect of static bed height on methane combustion efficiency, predicted by the present model. The methane combustion efficiency increased as the static bed height increased in the fuel reactor. The retention time of gas and particles increases as static bed height increases. That seems to result in the increase of combustion efficiency. The present result agrees with that of Abad et al. [5] on the effect of bed weight. However, the combustion efficiency did not seem to get 100% at static bed height <0.45 m with any solids circulation rate. The minimum solids circulation rate required for complete combustion in Fig. 3(b) decreased exponentially with an increase of static bed height of the fuel reactor. The required fresh feed rate of OC particles in Fig. 3(c) was predicted to increase as the static bed height increased, because the particle attrition rate increases with an increase of static bed height [14].

Fig. 4(a) shows the effect of static bed height on methane combustion efficiency when total bed mass of both reactors is set constant, predicted by the present model. Change of bed mass in both reactors is interrelated with each other in this case. The bed height of the fuel reactor increases fast as the bed height of the air reactor decreases slowly because the cross-sectional area of the air reactor is bigger than that of the fuel reactor. The combustion efficiency is predicted to increase as the static bed height increases in the fuel reactor. The minimum solid circulation rate required for complete combustion in Fig. 4(b) decreased exponentially with an increase of static bed height of the fuel reactor. Those results shown in Fig. 4(a, b) are similar to the results shown in Fig. 3(a, b). The present result agrees partly with that of Kolbitsch et al. [8] on the effect of solids inventory shifting. They showed that the CH_4 slip increased after an initial decrease as the solids inventory of the air reactor in-

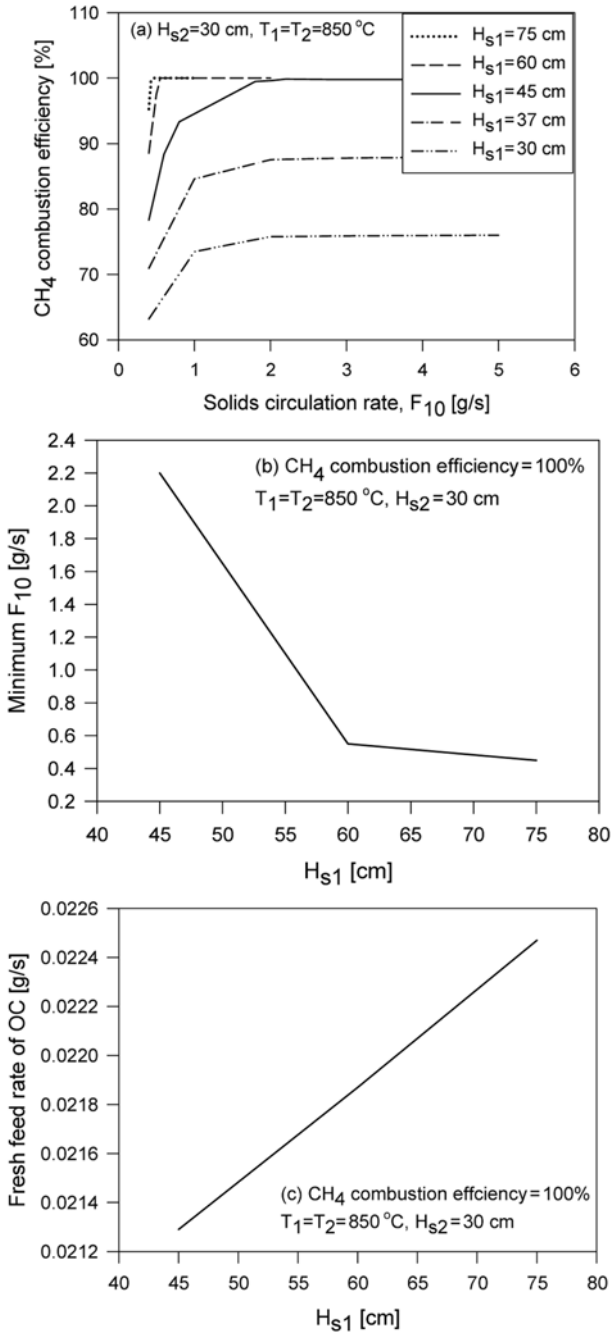

Fig. 3. Effect of static bed height on performance of CLC, calculated by the present model.

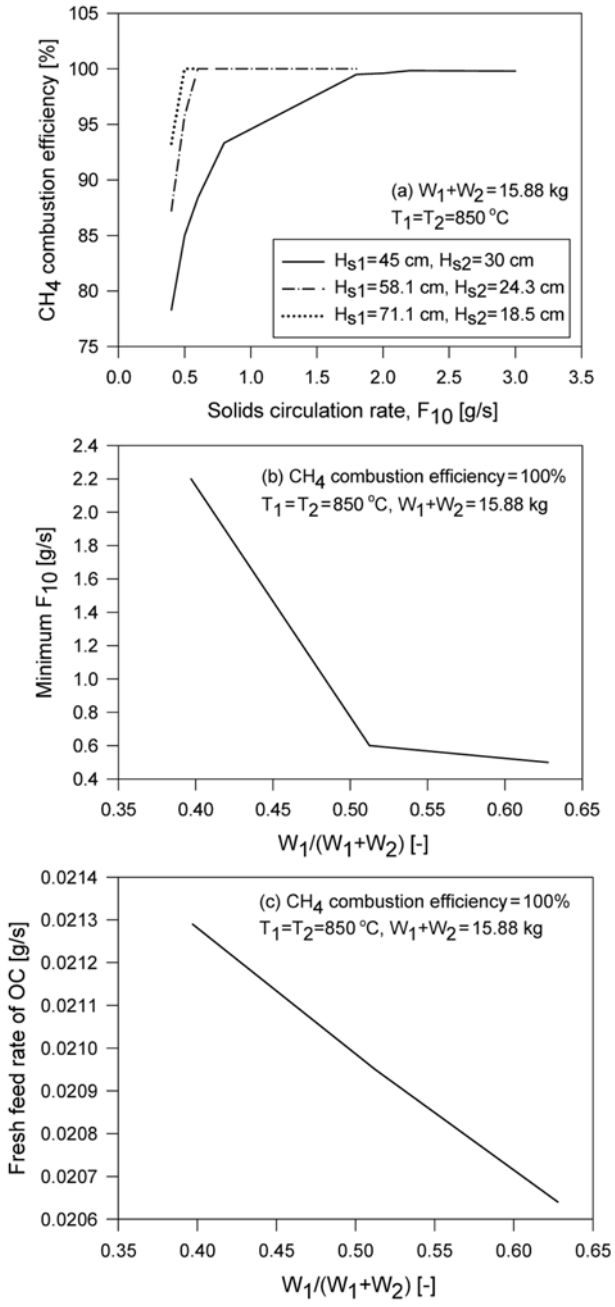

Fig. 4. Effect of the ratio of fuel reactor bed mass to total bed mass on performance of CLC, calculated by the present model.

creased. The minimum CH_4 slip occurred at a ratio of solids inventory of the fuel reactor to the total solids inventory between 0.4 and 0.6. In this range, the change of CH_4 slip was as slow as the solid circulation rate shown in Fig. 4(b) for complete combustion between 0.51 and 0.63 in ratio of solids inventory of the fuel reactor to the total solids inventory. The required fresh feed rate of OC particles in Fig. 4(c) was predicted to decrease a little, quite unlikely to Fig. 3(c), as the static bed height increased. It is because the particle attrition rate rather decreases since the static bed height of the air reactor that has the fluidizing gas velocity greater than that of the fuel reactor decreases [14] in the present process.

CONCLUSIONS

We developed a practical model to predict performance of a bubbling fluidized-bed CLC system for methane. The model reflects such particle conditions as wide size distribution, particle attrition, formation of fine particles by attrition, resultant loss of fine particles by elutriation and makeup of fresh particles. The present model provides a reasonable fit to experimental results on methane combustion efficiency. The operation condition of CLC system is determined by the range of OC solids circulation rate in which complete combustion achieved. The minimum circulation rate of OC particles for complete combustion decreases within the considered oper-

ation condition as temperature or bed mass increase in the fuel reactor. Large bed mass is required to get complete combustion with low temperature in the fuel reactor. The fresh feed rate of OC particles increases in complete combustion condition as temperature or static bed height or gas velocity increase. Further comparison of simulation results with experimental data is desirable in the future.

ACKNOWLEDGEMENTS

This work was supported by the Power Generation & Electricity Delivery of the Korea Institute of Energy Technology Evaluation and Planning (KETEP) grant funded by the Korea government Ministry of Knowledge Economy (2009101010010A).

NOTATION

b_i : stoichiometric constant for reaction i [-]
C'_{io} : C'_i at h=0 [kg mol/m^3]
C'_{if} : C'_i at bed surface [kg mol/m^3]
C'_i : average concentration of gaseous reactant in reactor i [kg mol/m^3]
E_i : activation energy of reaction i [J/kg mol]
F_j : solid flow rate of stream j [kg/s]
H_{si} : static bed height of reactor i [m]
K_a : particle attrition rate constant [1/m]
k_{oi} : frequency factor of reaction i [m$^{3n_i-2}$/kgmol$^{n_i-1}$s]
$K_i^*(x)$: particle elutriation rate from bed i [kg/s]
$m_{NiO,i}$: formed (i=2) or disappeared (i=1) NiO in reactor i [kg mol/s]
m_i : consumption of gaseous reactant (CH_4 or O_2) in reaction i [kg mol/s]
n_i : order of reaction i [-]
$p_{ai}(x)$: probability density function of particles formed by attrition in bed i [1/m]
$p_{bi}(x)$: probability density function of particles in bed i [1/m]
$p_j(x)$: probability density function of particles in stream j [1/m]
$p_0(x)$: probability density function of fresh feed particles [1/m]
R : gas constant, 8.314 [kPa m^3/kg mol K]
R_{ai} : overall formation rate of fine particles by attrition in bed i [kg/s]
$R_{f1\backslash 2}$: recycle fraction of solid collected by fuel reactor's cyclone to fuel reactor [-]
R_{f2} : recycle fraction of solid collected by air reactor's cyclone to air reactor [-]
$R_i(x)$: particle attrition rate in bed i [m/s]
S_{ij} : mass flow rate of total particle in outflow stream i from bed i [kg/s]
t : time [s]
T_i : temperature of reactor i [K]
u_i : fluidizing velocity in reactor i [m/s]
u_{mfi} : minimum fluidizing velocity in reactor i [m/s]
W_i : weight of bed i [kg]
x : spherical particle diameter [m]
X_i : conversion of solid reactant (NiO or Ni) for reaction i [-]
x_{max} : maximum particle diameter [m]

Greeks

α_{ik} : functions defined as Eqs. (2a, b) [1/m]
α_{i3} : function defined as Eq. (2c) [1/m^2]
γ_i : mole of solid reactant per volume of particle in reactor i [kg mol/m^3]
δ_{ij} : Kronecker delta, one at i=j and zero at i≠j[-]
η_i : correction factor for reaction i [-]
ρ_B : mole Ni per mass of fresh particle [kg/m^3]
ρ_p : particle density [kg/m^3]
$\tau_i(x)$: mean particle residence time in reactor i [s]
ϕ : fraction of active Ni for oxygen carrier particle [-]
$\psi_i(x)$: fractional particle collection efficiency of cyclone i [-]
$\varpi_{bi}(x)$: mass fraction of particle in bed i [-]
$\varpi_{ij}(x)$: mass fraction of particle in outflow stream j from bed i [-]

Subscripts

i : free index, 1 for fuel reactor or reduction of NiO or CH_4; 2 for air reactor or oxidation of Ni or O_2
j, k : dummy indices

REFERENCES

1. S. Balaji, J. Ilic, B. E. Ydstie and B. H. Krogh, *Ind. Eng. Chem. Res.*, **49**, 4566 (2010).
2. Z. Deng, R. Xiao, B. Jin, Q. Song and H. Huang, *Chem. Eng. Technol.*, **31**, 1754 (2008).
3. J. Jung and I. K. Gamwo, *Powder Technol.*, **183**, 401 (2008).
4. A. Abad, J. Adanez, F. Garcia-Labiano, L. F. de Diego and P. Gayan, *Energy Procedia*, **1**, 391 (2009).
5. A. Abad, J. Adanez, F. Garcia-Labiano, L. F. de Diego and P. Gayan, *Combust. Flame*, **157**, 602 (2010).
6. J. Bolhàr-Nordenkampf, T. Proell, P. Kolbitsch and H. Hofbauer, *Chem. Eng. Technol.*, **32**, 410 (2009).
7. Z. Deng, R. Xiao, B. Jin and Q. Song, *Int. J. Greenhouse Gas Control*, **3**, 368 (2009).
8. P. Kolbitsch, T. Proell and H. Hofbauer, *Chem. Eng. Sci.*, **64**, 99 (2009).
9. I. Iliuta, R. Tahoces, G. S. Patience, S. Rifflart and F. Luck, *AIChE J.*, **56**, 1063 (2010).
10. H. Kruggel-Emden, S. Rickelt, F. Stepanek and A. Munjiza, *Chem. Eng. Sci.*, **65**, 4732 (2010).
11. C. E. Lapple, *Chem. Eng.*, **58**, 144 (1951).
12. D. Kunii and O. Levenspiel, *Fluidization engineering*, 2nd Eds., Butterworth-Heinemann, Boston, U.S.A. (1991).
13. J. H. Choi, C. K. Yi and S. H. Jo, *Korean J. Chem. Eng.*, **28**, 1144 (2011).
14. D. Merrick and J. Highley, *AIChE Symp. Ser.*, **70**, 366 (1974).
15. J. Werther and J. Reppenhagen, *AIChE J.*, **45**, 2001 (1999).
16. C. Y. Wen and Y. H. Yu, *AIChE J.*, **12**, 610 (1966).
17. H.-J. Ryu, P. S. Yoon and J.-H. Choi, in *Abstracts for 2010 Korea institute of chemical engineering fall meeting*, 275 (2010).
18. Y.-W. Jeon, *Hydrodynamic and oxidation-reduction reaction characteristics of oxygen carrier particles in an annular type chemical looping combustor*, Master Thesis, Korea Advanced Institute of Science and Technology, Daejeon, Korea (2010).